IOSR Journal of Mechanical and Civil Engineering (IOSR-JMCE)
e-ISSN: 2278-1684,p-ISSN: 2320-334X, Volume 15, Issue 4 Ver. IV (Jul. - Aug. 2018), PP 62-70
www.iosrjournals.org

Interaction Effect on Hydro-dynamic Performance of a Rudder - Propeller System

Nguyen Chi Cong[1,2], Pham Thi Thuy[1], Vu Van Duy[1], Luong Ngoc Loi[2] and Ngo Van He[2]

[1]*Vietnam Marine University, 180000, Haiphong, Vietnam*
[2]*Hanoi University of Science and Technology, 10000, Hanoi, Vietnam*
Corresponding Author:NgoVan He

Abstract: *The use of Computational Fluid Dynamics (CFD) to predict internal and external flows has risen dramatically in the past decade. The widespread availability of engineering workstations together with efficient solution algorithms and sophisticated pre - and post-processing facilities enable the use of commercial CFD codes by graduate engineers for research, development and design tasks in industry. In the ocean engineering in which the cost of experiment is dramatically high, or sometime the experimental method is impossible to employ, it becomes the vital tool in designing and optimizing the shape of vessels and propulsion. In this topic, authors used the commercial software, ANSYS-Fluent v.14.5, to illustrate the effects of rudder and propeller on hydrodynamics performances of the marine propeller. The first objective of the paper uses the numerical method to analyze and build the characteristic curves of marine propeller. The second aim is to study how the rudder affects the hydrodynamic feature of the propeller in ship operation. The marine propeller used in this work has designed conditions as follows: the diameter of 3.65m; speed of 200rpm; average pitch of 2.459m; boss ratio of 0.1730. Using the CFD, the characteristic curves of the marine propeller and others CFD results as well as pressure, velocity distribution around propeller and efficiency of the propeller are presented. From result of comparison at other CFD results, the interaction effect on hydro-dynamic performances of the rudder – propeller system is investigated. The obtained outcomes of this paper are the significant foundation to calculate and design of an innovative kind of propulsion for ships with high performances.*

Keywords:*CFD, rudder, propeller, hydro-dynamic, interaction effect.*

Date of Submission: 23-08-2018 Date of acceptance: 23-08-2018

I. Introduction

The interaction effects between the propeller wake and the rudder is an intricate question for propulsion and ship designers in many decades, it being related to the hydrodynamic performance of the ship, structural vibrations, noise emission, as well as control of the course and maneuverability. Therefore, efficient improvement of a propulsion system is a crucial demand, and numerical methods are able to investigate the hydrodynamic behaviour of them. To pay attention to the problem, there are obtained achievements as follows:

In 2003, Takayuki. W used the RANS solver, and the hybrid grid system to investigate flow around a propeller with cavitation and no cavitation. The gained results ofhis research reveals that the CFD simulation results were in good agreement with the experiment, and without depending on the type of mesh [1]. The RANS method was also used to study the propeller sheet cavitation and propeller-ship interaction (J. Bosschers. At al 2008) [2]. In 2017, at 10th International conference on marine technology,Arnob.Bgot some results relating computation of hydrodynamic characteristic of marine propeller using induction factors method base on normal induced velocity[3]. The significant results were that the normal induced velocity of a propeller can be obtained simply and accurately by means of the induction factors. In the same year at this conference, Karim at al employed the numerical method to calculate flow field around ship hull including self-propulsion characteristics at varying rudder positions. The main conclusion of their paper is: Zonal approach for computing flow characteristics is more effective than global approach in regard to both time and expense, various hydrodynamic characteristics of ships and propellers show good agreement with available experimental results and Lifting line method coupled withRANSsolver can be used effectively to determine self-propulsion characteristics of marine propellers at changing rudder positions. The effect of rudder decreases with the increase in distance of rudder position from the propeller[4]. To pay attention to this discipline, some authors has also taken some significant results stated in [5-9]

In the present study, the authors employed the numerical method to predict the hydrodynamic performance of the propeller-rudder system, investigate effects of a rudder on pressure distribution and thrust of

each blade. Moreover, the velocity changes of flow going through the propeller, and the pressure distribution at different radii are also discussed in a detail way. The last, the effects of a propeller on a rudder's hydrodynamic features and a ship's maneuver are presented and discussed.

II. Mathematical foundation

2.1 Hydrodynamic performance of a propeller

In analysis of a marine propeller, we use significant non-dimension coefficients that are thrust, torque, efficiency coefficient. they are functions of advance ratio and can be defined as follows [10].

$$K_T = \frac{T}{\rho n^2 D^4}; K_Q = \frac{Q}{\rho n^2 D^5}; J = \frac{V_a}{nD}; \eta_0 = \frac{K_T.J}{K_Q.2\pi} \quad (1)$$

Where:

V_A is advance velocity, J is advance ratio, n is rotational velocity, D is propeller diameter, T is total thrust, ρ is water density and Q indicates total torque.

2.2 Hydrodynamic characteristics of rudder

The horizontal sectional shape of the rudder is symmetric and just same as wing sections of airplane. The rudder generates force by the steered angle. The force is usually defined as the normal force $F_N$acting on the rudder's symmetrical plane and shown as follows [10]:

$$F_N = \frac{1}{2} c_N . \rho V_\infty^2 . A \quad (2)$$

Here:

α is the incident angle of inflow to the rudder that is made by rudder steered angle and the resultant flow of propeller slip stream and ship turning motion.

c_N is the normal force coefficient of the rudder section as a wing being the function of the the incident angle of inflowα.

A is the acting area of the rudder.

V_∞ is the inflow velocity coming up the rudder.

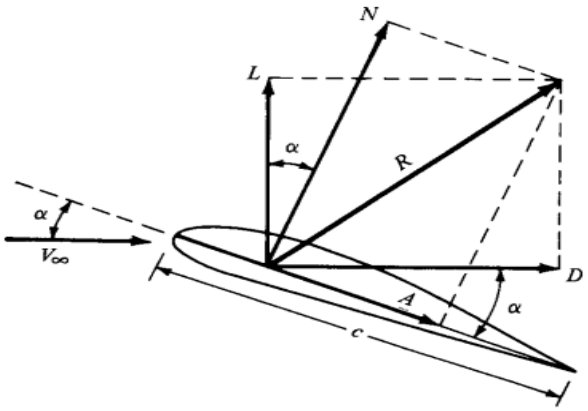

Figure 1: Hydrodynamic fore acting on a rudder

2.3 Theoretical CFD basis

In fluid mechanic, there are three basic conservation laws: conservation of mass, conservation of momentum and conservation of energy. Because flow around a marine propeller is a low speed, incompressible fluid flow and the temperature difference between body and fluid is assumed to be small, the conservation of energy is excluded. Therefore, in investigating a marine propeller, we use two fundamental conservation principles: mass and momentum principle. In the moving reference frame, they are written as follows [11]:

- Conservation of mass:

$$\frac{\partial \rho}{\partial t} + \nabla . \rho \vec{v}_r = 0 \quad (3)$$

- Conservation of momentum:

The conservation of momentum equation is acquired when Newton's second law is applied to a fluid particle with assumption that fluid is continuous, isotropic and linear viscous. It is so called Navier Stokes (NS) equation, written in rotating coordinate system as follows.

$$\frac{\partial}{\partial t}(\rho\vec{v}_r)+\nabla.(\rho\vec{v}_r.\vec{v}_r)+\rho(2\vec{\omega}\times\vec{v}_r+\vec{\omega}\times\vec{\omega}\times\vec{r}+\vec{a}\times\vec{r}+\vec{a})=-\nabla p+\nabla\bar{\bar{\tau}}+\vec{F} \quad (4)$$

Where $\vec{a}=\frac{d\vec{\omega}}{dt}$ and $\vec{a}=\frac{d\vec{v}_t}{dt}$

The stress tensor $\bar{\bar{\tau}}$ is given by:

$$\bar{\bar{\tau}}=\mu\left[\left(\nabla\vec{v}+\nabla\vec{v}^{T}\right)-\frac{2}{3}\nabla\vec{v}I\right] \quad (5)$$

III. Calculation models and boundary condition

3.1 Problem geometry and domain

In this paper, the rudder-propeller system of the container TanCang foundation ship was investigated. The main parameters of the propeller and rudder are presented in the table 1 and 2.

Table 1: Propeller detailed parameters

Name	Value	Unit
Diameter	3.65	m
Pitch	2.459	m
Revolution	200	rpm
Number of blade	4	
Rake	10	Degree
Screw	25	Degree
Cross section	Naca66, a=0.8	
Diameter	3.65	m

Table 2: Propeller detailed parameters

Name	Value	Unit
Rudder height	4,8	m
Chord length of top	3,45	m
Chord length of bottom section	2.45	m
Rudder area	12	m^2
Rudder profile	NaCa 0018	

3.2 Geometry and computed fluid domain

In the first step of the project, the SolidWork software was employed to build the propeller -rudder geometry and fluid domain, suitable space surrounding the rudder propeller system. The domain is the cylinder with diameter of 7 D, the length of 13 D and was divided in two components: the dynamic domain and dynamic domain[12-15]. The next step, the team used the ICEM meshing tool to mesh and refine for all domains. The dynamic domain with small mesh, and the static domain with the coarse mesh are shown in the figure 2. To determine the reasonable number of mesh for all calculations, the six cases were carried out and then finally authors chose the five-case mesh number for all simulations. The geometry and mesh details are shown in the table 3 and figure 2.

Table 3. Mesh details forsimulation

Domain	Nodes	Elements	Polyhedral
Dynamicfluid	1649594	326437	326437
Staticfluid	1968607	356299	356299

All Domains	3618201	682736	682736

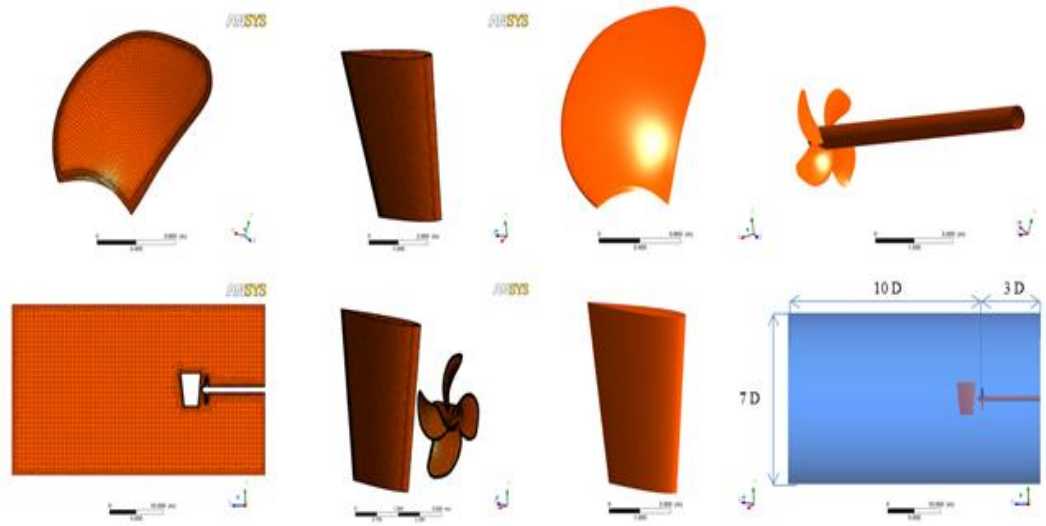

Figure 2: Geometry and mesh for computations

Figure 2: Geometry and mesh for computations

3.3 Calculation method and boundary conditions

The RNG k - ε two - equation model is chosen as the turbulence model to close Reynolds averaged equations velocity inlet is selected as inlet boundary condition [11]. Inlet is set velocity inlet with the assumption that flow is uniform at axis direction and its value equals to the advance velocity of the ship. Pressure outlet is specified as the outlet boundary condition, and gauge pressure on the outlet is set to be 0 pa. As to wall boundary condition, no slip condition is enforced on wall surface and standard wall function is also applied to adjacent region of the walls. Moving reference frame (MRF) is used to establish the moving coordinate system rotating with thepropeller synchronously and the stationary coordinate system fixed on static shaft of the propeller, respectively. The first order upwind scheme with numerical under- relaxation is applied for the discretization of the convection term and the central difference scheme is employed for the diffusion term. The pressure - velocity coupling is solved through the PISCO algorithm. Convergence precision of all residuals is under 0.0001. The details of boundary conditions are shown in the table 4 below.

Table 4: Boundary conditions

Name	Conditions	Value	Units
Inlet	Velocity inlet		m/s
Outlet	Pressure outlet	0	Pa
Wall	Static wall	-	
Blade	Rotational wall	0	Rpm
Hub	Rotational wall	0	Rpm
Static shaft	Static wall	-	
Static domain	Static fluid	-	

IV. Results and discussion

4.1. Hydrodynamic performance of the propeller

The figure 3 describes the pressure distribution on the back face and pressure face of the propeller at the advance ratio of 0.1 and 0.6. It is clear from this figure that pressure value of the pressure face is higher than back face. As a consequence, the fluid toward the suction side is attracted because of the low pressure on this face to make the flow accelerate, and the fluid continues accelerating at the pressure face because of high

pressure on it. The propeller's thrust is made due to the pressure difference between the propeller-blade faces. Moreover, when the advance ratio J goes up, the pressure difference of the blade's faces of the propeller goes down. At the advance ratio J of 0.1, almost area of the pressure face has value in the range of 4.10^4 -$1.2.10^5$ Pa, and almost area of the back face gets value in the range of -$1.2.10^5$ - -4.10^4 Pa. In contrast, at the advance ratio J of 0.6, these pressure values of pressure and back face is in the range of $2.4.10^4$ Pa - 4.10^4 Pa and -$2.4.10^4$ Pa - -$7.2.10^4$ Pa respective. Because of this reason, the propeller thrust dropped consistently when the advance ratio J goes up, the Z force distribution on the blade's face at the advance ratio J of 0.1 and 0.6 is presented in the figure 4.

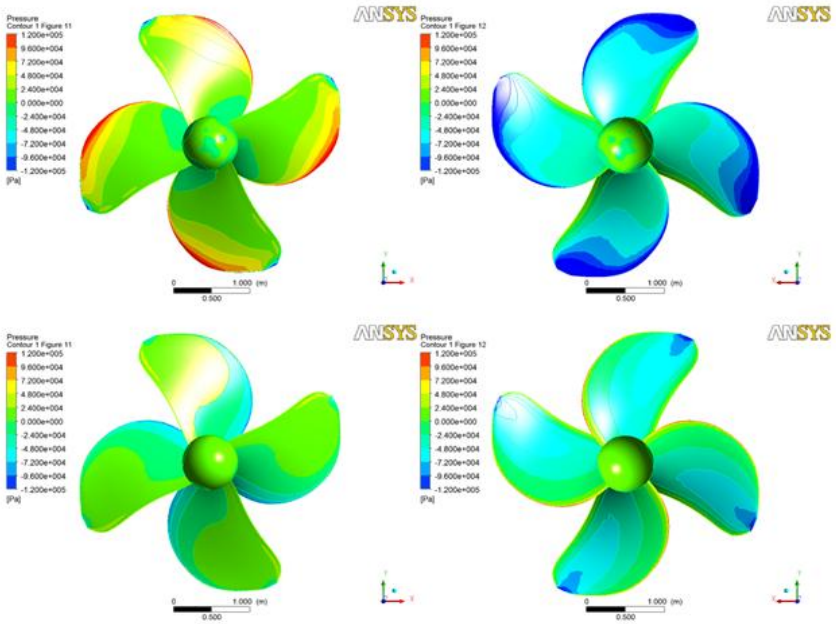

Figure 3: Pressure distribution on pressure faces of the propeller at J =0.1, 0.6

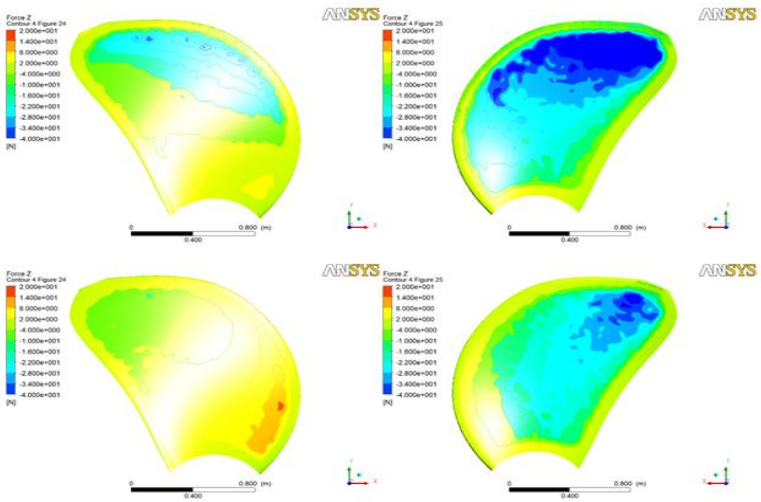

Figure 4: Distribution of Z force on a blade's faces of the propeller.

The propeller's hydrodynamic performance is shown in the figure 8. We can see from the figure that thrust and torque coefficients is the nearly linear function of advance ratio J and their maximum in this research is 0.283, and 0.031 corresponding with the advance ratio of 0.1. In a different way, the propeller's efficiency is a curve of the advance ratio J and it is nearly linear with the small speed. The efficiency of propeller steadily increases when the velocity in let goes up, the maximum efficiency taken is 0.714 at the advance ratio J of 0.6.

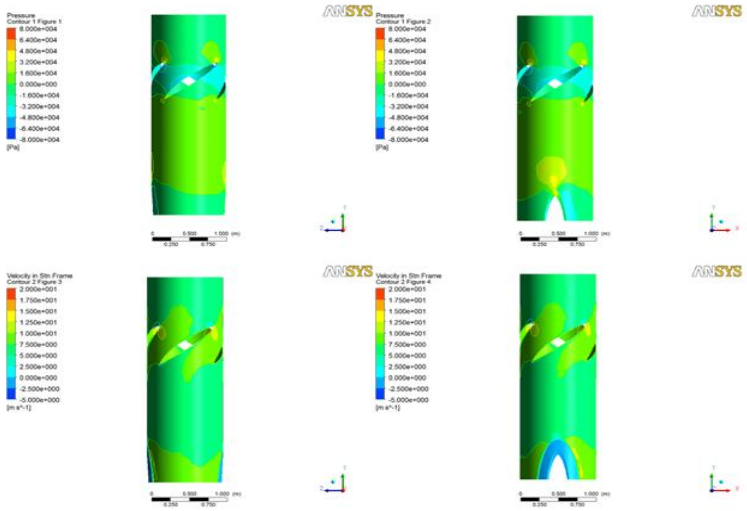

Figure 5: Pressure and velocity distribution at radius of 0.5m

Velocity and pressure distribution at the radius of 0.5 corresponding with the advance ratio of 0.6 is presented in the figure 5. It can be seen from the figure that the pressure distribution principle of profiles obeys the thin airfoil theory[16-18]. The value pressure of pressure faces is higher than that of the suction faces, and it gets the maximum at the leading edge. However, this distribution is slightly different with the theory due to together effects of other airfoils on the net. Moreover, from the velocity distribution, we can see that fluid accelerates when going through the space between two blades called a propeller channel. It gets the maximum about 15 m/s at the first channel, slowly decreases in the channel because of the channel expansion. At the end of the channel, the fluid gets value about 12 m/s.

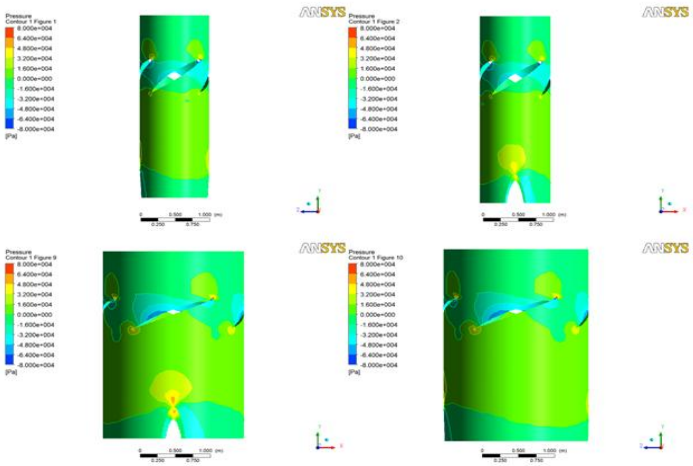

Figure 6: Pressure distribution at radius of 0.5 and 1m

Pressure distribution at radii is presented in the figure 6. As can be seen from this figure that pressure distribution on a profile in net at small radii is relatively uniform. At the larger radii, there is a considerable difference in pressure distribution among profile due to propeller's geometry and rudder shape and interaction between propeller and rudder in operation. This makes difference of pressure distribution among blade, and causes the difference in thrust among the blades.

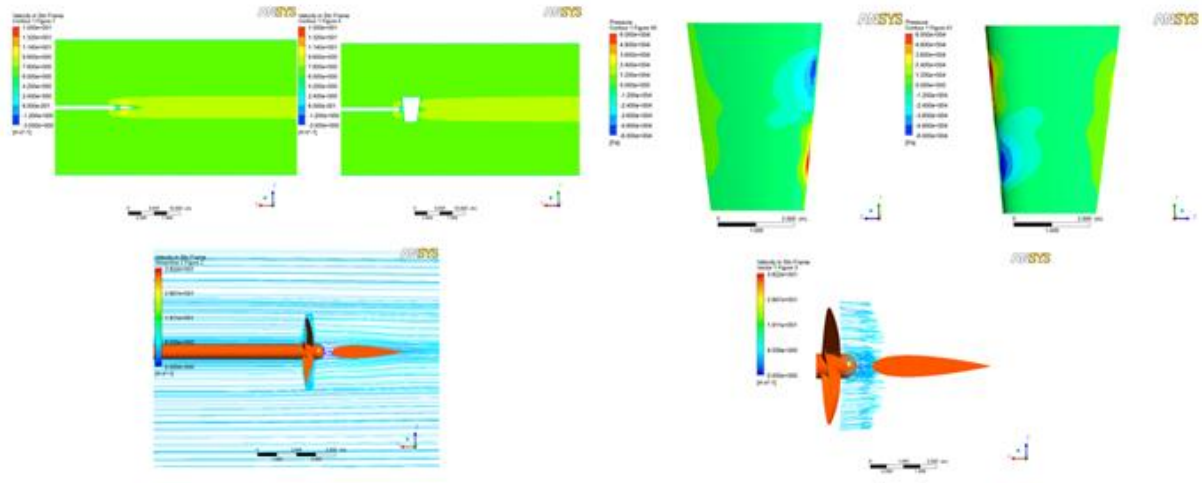

Figure 7: Velocity distribution on axial plane at J =0.6

The figure 7 displayed the velocity distribution on the axial plane at the advance ratio J of 0.6. As can be seen from the figure that velocity increases after going out the propeller and the maximum velocity in this case is 11 m/s. The flow at the region between the hub and the rudder is the turbulent flow with the negative velocity, the velocity at this area is about -2 m/s. The area is easier to get cavitation because the pressure of it is lower than that of other regions.

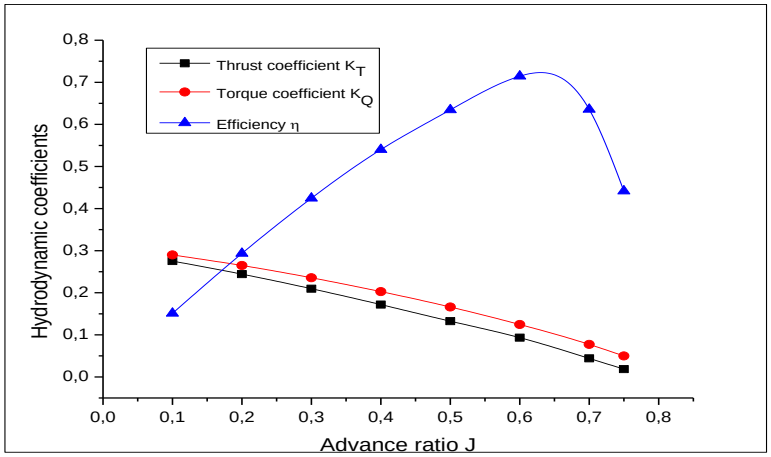

Figure 7: Characteristic curves of the propeller

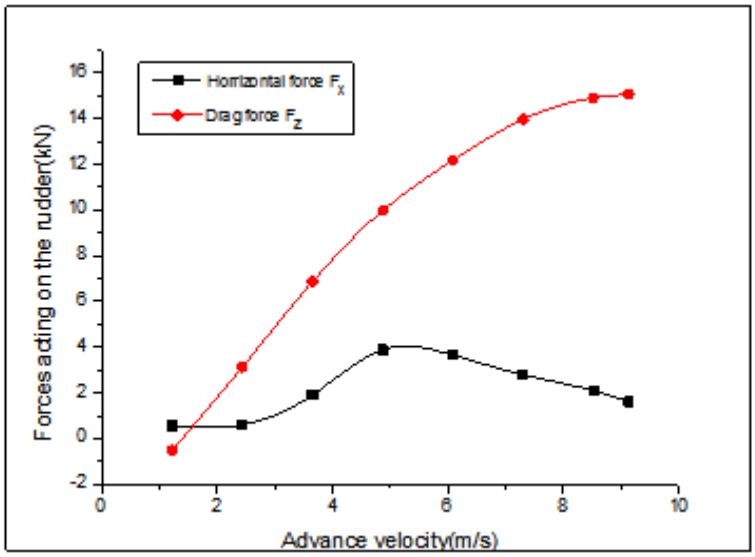

Figure 8: Forces acting on the propeller at different ratios

4.2. Hydrodynamic features of the rudder

The figure 5 presented the vector velocity going out the propeller, and pressure distribution of the rudder's faces. It can be seen from this figure that velocity field after the propeller is not uniform, and flow's vector incline with the rudder's symmetry plane with any angle. This made pressure distribution of rudder faces is asymmetric and the maximum pressure gets about 6.10^4 Pa at the region corresponding with the propeller's blade tips. As a results, it is not only the drag on the rudder but only the vertical force appearing on the rudder. The rudder's drag changes in a nearly linear function of advance ratio J, and the maximum drag of the rudder is 16kN at the advance ratio J of 0.75. On the other hand, the vertical force is a curve of advance ratio J, it gets the maximum value about 4kN corresponding with J of 0.5. At the small velocity, it increases dramatically, while at the advance ratio J in the range of 0.5 - 0.75, it decreases slightly. The changing principle of forces is given in the figure 9.

4.3. Effects of interaction between the propeller and therudder on the ship's maneuver

From the simulation results, we can recognize that in the ship operation the forces acting on the rudder are not only the drag but also the horizontal force. The magnitude of the horizontal force depends on the advance velocity of the ship and the angular velocity of the propeller. The forces and vorticity generating by the interaction of the rudder and propeller make the ship moving the in zigzag routine

V. Conclusion

In this study, numerical investigation and analysis of steady flows for the rudder- propeller at the different ratios have been presented. A unstructured grid based on RANS andthe RNG k-ε turbulent model are applied to investigate the hydrodynamic performance of propeller and the interaction between the propeller and the rudder

- The four-bladed skewed propeller of the TanCang foundation ship is selected to simulate and construct the propeller's open water performance curves. The numerical predictions of K_T, K_Q , η are also presented: the maximum thrust, torque, efficiency coefficients are 0.31, 0.028 and 0.714 respectively.
- The change's velocity and pressure of flow going in the space between two blades of the propeller also discussed. The pressure distribution of profiles at the small radius are relatively uniform, and the other profiles at the larger radius are quite different because of the rudder and propeller geometry and the interaction between them. This difference makes thrust among the propeller's blade to be not equal, and causes the propeller's oscillation in operation. In addition, the flow's velocity in the space between two blades is suitable with the turbomachinery theory, and the maximum velocity of fluid gets about 15 m/s at the first part of the channel due to the low pressure on the suction face of the propeller and the reduction of the channel.
- Because of the interaction between the propeller and rudder, forces acting on the rudder is not only the drag but also the horizontal force. The rudder's drag changes have the linear principle with advance velocity and gets the maximum value at J of 0.75. The horizontal force has the complex changing principle with advance velocity and obtains the maximum value of 4 kN at advance ratio J of 0.4. This forces is a cause to make the ship going to sea with a zigzag routine.

- The unequal thrust made on each blade of the studied propeller due to the interaction between the propeller and the rudder is discussed. The rudder makes slight change in pressure distribution of the propeller's blades from which it makes the unequal forces on each blade. The thrust difference on propeller's blade make it oscillate in operation.

References

[1]. Takayuki WATANABE, T.K., Masatsugu MAEDA, Shin Hyung RHEE, Simulation of steady and unsteady cavitation on a marine propeller using a rans cfd code, in Fifth International Symposium on Cavitation. 2003.
[2]. J. Bosschers, G.V., A.R. Starke, E. van Wijngaarden, Computational analysis of propeller sheet cavitation and propeller-ship interaction, in RINA conference "MARINE CFD2008. 2008: Southampton, UK.
[3]. Banik, A. and M.R. Ullah, Computation of Hydrodynamic Characteristics of A Marine Propeller Using Induction Factor Method Based on Normal Induced Velocity. Procedia Engineering, 2017. 194: p. 120-127.
[4]. Karim, M.M. and N. Naz, Computation of Flow Field around Ship Hull including Self Propulsion Characteristics at Varying Rudder Positions. Procedia Engineering, 2017. 194: p. 96-103.
[5]. Liu, D., The Numerical Simulation of Propeller Sheet Cavitation with a New Cavitation Model. Procedia Engineering, 2015. 126: p. 310-314.
[6]. Praveen Kumar, K.M., Analysis of Marine Propulsor in Crashback using Large Eddy Simulation, in Fourth International Symposium on Marine Propulsors. 2015: Austin, Texas, USA. p. 9.
[7]. Shuai Sun, X.C., Chao Wang, Tao Mo, Research on the Optimization Design of Propeller Considered the Off-designed Conditions, in International Industrial Informatics and Computer Engineering Conference. 2015.
[8]. Stefano Gaggero, M.V., Juan Gonzales Adalid, Mariano Perez Sobrino, and M.S. Giulio Gennaro, Gianluca Bina, A Design by Optimization of Tip Loaded Propellers, in Fourth International Symposium on Marine Propulsors. 2015: Austin, Texas, USA.
[9]. Amir Hossein Razaghian, H.G., Numerical analysis of the hydrodynamic characteristics of the accelerating and decelerating ducted propeller. Scientific Journals of the Maritime University of Szczecin, 2016.
[10]. Carlton, J.S., Marine Propellers and Propulsion, ed. 2. 2007. 556.
[11]. ANSYS Fluent Theory Guide. 2013: p. 814.
[12]. Abramowicz-Gerigk, T., Distribution of flow velocity generated by propellers of twin propeller vessel. Scientific Journals Maritime University of Szczecin, 2010: p. 8.
[13]. Alejandro Caldas, M.M., AdriánSarasquete, Numerical Analysis of Rudder Effects upon Ducted Propeller Units, in Second International Symposium on Marine Propulsors. 2011: Hamburg, Germany.
[14]. Ghassemi, H. and P. Ghadimi, Hydrodynamic efficiency improvement of the High Skew Propeller for the underwater vehicle under surface and submerged conditions. Journal of Ocean University of China, 2011. 10(4): p. 314-324.
[15]. Lu, L., G. Pan, and P.K. Sahoo, CFD prediction and simulation of a pumpjetpropulsor. International Journal of Naval Architecture and Ocean Engineering, 2016. 8(1): p. 110-116.
[16]. John D, A., Jr, Fundamental of aerodynamics. Mc Graw-hill.
[17]. John P. Breslin, P.A., Hydrodynamics Of Ship Propellers. 1994: Cambridge university press.
[18]. IRA H. ABBOTT, A.E.V.D., Theory of wing sections. 1959.

NgoVan He "Interaction Effect on Hydro-dynamic Performance of a Rudder - Propeller System." IOSR Journal of Mechanical and Civil Engineering (IOSR-JMCE) , vol. 15, no. 4, 2018, pp. 62-70